

See discussions, stats, and author profiles for this publication at: <https://www.researchgate.net/publication/328832013>

# Gas switching reforming (GSR) for power generation with CO<sub>2</sub> capture: Process efficiency improvement studies

Article in *Energy* · November 2018

DOI: 10.1016/j.energy.2018.11.023

CITATIONS

8

READS

79

4 authors:



**Shareq Mohd Nazir**

KTH Royal Institute of Technology

14 PUBLICATIONS 54 CITATIONS

[SEE PROFILE](#)



**Jan Hendrik Cloete**

SINTEF

33 PUBLICATIONS 111 CITATIONS

[SEE PROFILE](#)



**Schalk Cloete**

SINTEF

116 PUBLICATIONS 853 CITATIONS

[SEE PROFILE](#)



**Shahriar Amini**

SINTEF

115 PUBLICATIONS 848 CITATIONS

[SEE PROFILE](#)

Some of the authors of this publication are also working on these related projects:



Filtered Two Fluid Models (fTFMs) for industrial-scale fluidized bed reactor simulations [View project](#)



A Multi-scale Simulation-Based Design Platform for Cost-Effective CO<sub>2</sub> Capture Processes using Nano-Structured Materials -NanoSim [View project](#)

# Gas switching reforming (GSR) for power generation with CO<sub>2</sub> capture: Process efficiency improvement studies

Shareq Mohd Nazir<sup>a\*</sup>, Jan Hendrik Cloete<sup>a</sup>, Schalk Cloete<sup>b</sup>, Shahriar Amini<sup>a,b</sup>

<sup>a</sup>Department of Energy and Process Engineering, Norwegian University of Science and Technology, Trondheim, Norway

<sup>b</sup>SINTEF Industry, Trondheim, Norway

## Abstract

This paper presents the process improvement studies of a combined cycle power plant integrated with a novel gas switching reforming (GSR) process for hydrogen production with integrated CO<sub>2</sub> capture. The overall process is denoted as GSR-CC (gas switching reforming-combined cycle). Five cases are presented in which a systematic approach was adopted to improve the net electrical efficiency of the GSR-CC process. Two cases focus on reducing the number of unit operations and the other three cases focus on heat integration. The net electrical efficiency of the base case GSR-CC process is 45.8% whereas the improved GSR-CC has a net electrical efficiency of 51.1%. The efficiency penalty in the improved GSR-CC process is only 7.2 %-points with respect to the reference case natural gas combined cycle power plant without CO<sub>2</sub> capture, and is less than post-combustion capture methods presented in literature. The CO<sub>2</sub> avoidance in the GSR-CC is more than 95%. GSR-CC also gives a flexibility in the output from the plant in terms of pure H<sub>2</sub> or electricity and the optimal plant configuration is designed to maximize this flexibility.

\*Corresponding author

Email: [shareq.m.nazir@ntnu.no](mailto:shareq.m.nazir@ntnu.no)

Telephone: +47- 48654776

Address: Kolbjørn Hejes vei 1b, Varmeteknisk\*A514, NTNU, NO-7491 Trondheim, Norway

**Keywords:** Gas-switching reforming; Pre-combustion capture; Combined cycle power plant; Net electrical efficiency; Process improvement; Heat integration.

## Nomenclature

CCS	Carbon Capture and Sequestration
CLC	Chemical Looping Combustion
CLR	Chemical Looping Reforming
CSTR	Continuous Stirred Tank Reactor
GSC	Gas Switching Combustion
GSR	Gas Switching Reforming
GSR-CC	Gas Switching Reforming–Combined Cycle
GT	Gas Turbine
HP	High Pressure
HRSG	Heat Recovery Steam Generator
LHV	Lower Heating Value
LP	Low Pressure
LPM	Lean Pre-mixed
MP	Medium Pressure
NG	Natural Gas
NGCC	Natural Gas Combined Cycle
PSA	Pressure Swing Adsorption
ST	Steam Turbine
TIT	Turbine Inlet Temperature
TOT	Turbine Outlet Temperature
WGS	Water Gas Shift
$\eta$	Net Electrical Efficiency

# 1 Introduction

The global electricity mix is still dominated by fossil fuels [1]. Coal, oil and gas satisfy nearly 82% of the primary energy demand as of 2014 [2]. Although the share of renewables is set to increase to 52% by 2060 in the proposed 2 °C scenario by the International Energy Agency (IEA), fossil fuels share will still be very significant [2]. Deployment of carbon capture and sequestration (CCS) technology is one of the ways to reduce CO<sub>2</sub> emissions but will also help in a smoother energy transition between fossil fuels and renewables [2].

The use of natural gas (NG) in power generation has significantly increased in the recent decades because NG based power plants possess higher net electrical efficiency and emit less CO<sub>2</sub> when compared to coal fired power plants. The use of NG is predicted to increase by 50% between 2014 and 2050 according to the central scenario presented in the World Energy Outlook 2016 [3]. Although NG based power plants emit less CO<sub>2</sub>, integrating CCS will be necessary to meet the targets set at the COP 21 meeting, to limit the global temperature rise to 1.5 °C [4].

CO<sub>2</sub> capture methods are broadly classified into three types: pre-, post-, and oxy-combustion. A detailed review of these capture methods is presented by Boot-Handford, Abanades [5] and Kenarsari, Yang [6] whereas the global status of deployment is presented in the report by GCCSI [7]. The focus of this paper is on a pre-combustion capture process in NG based power plant, where H<sub>2</sub> fuel is produced by a novel reforming method (gas switching reforming) and is used to fuel the gas turbine (GT).

Gas switching is based on the principle of chemical looping, which is gaining momentum for its ability to inherently separate CO<sub>2</sub> with no direct energy penalty. The two types of chemical looping systems that have been commonly reported in the literature are chemical looping combustion (CLC) [8, 9] and chemical looping reforming (CLR) [10]. A detailed review of these systems has been presented by Adanez, Abad [11]. In a NG based energy conversion process, CLC completely converts the chemical potential of NG into thermal energy, whereas CLR converts the chemical potential of NG into the chemical potential of the produced syngas, which can be further processed to yield H<sub>2</sub>. The exergy destruction in CLR is less when compared to conventional gas-gas partial oxidation reforming process [12].

One of the main challenges in CLR and CLC is the external circulation of oxygen carrier between the interconnected air and fuel reactors under pressurized conditions. To mitigate these challenges with chemical looping systems, a novel gas switching reactor concept was proposed and demonstrated experimentally [13, 14].

Figure 1 shows the schematic of the gas switching reforming (GSR) process. GSR has three steps: oxidation, reduction and reforming. During the oxidation step, compressed air is sent to the GSR to oxidize the metallic oxygen carrier and generate an oxygen depleted air stream (N<sub>2</sub>-rich stream), which has mainly N<sub>2</sub>. The oxygen carrier is then reduced by the off-gas from the pressure swing adsorption (PSA) unit to yield CO<sub>2</sub> and H<sub>2</sub>O in the reduction step. The NG is reformed with steam in the presence of oxygen carrier, which acts as a catalyst during the

reforming step. The endothermic reforming reaction is driven by the heat stored in the oxygen carrier from the highly exothermic oxidation step. The produced syngas is then further treated to produce pure H<sub>2</sub> via water-gas shift (WGS) and PSA units. The GSR process is dynamic in nature and hence needs a cluster of reactors with a coordinated operating strategy to produce syngas steadily. The process only involves switching modes of the gases and eliminates circulation of oxygen carrier between the reactors during each step of oxidation, reduction and reforming.

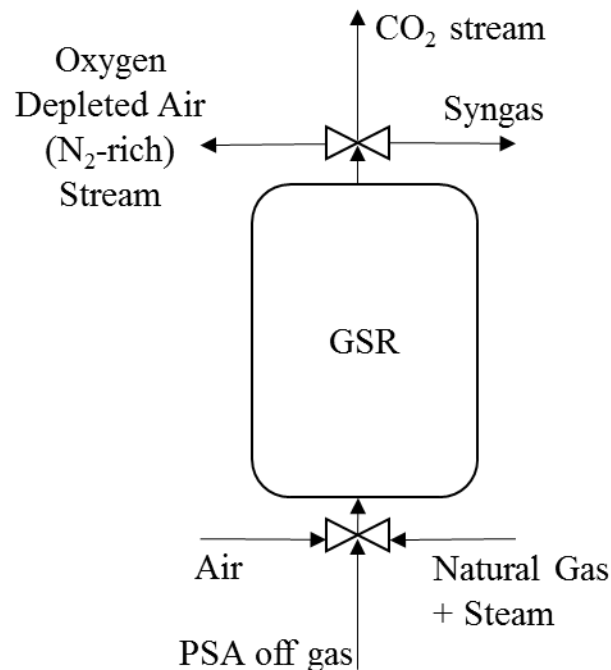


*Figure 1: Schematic of gas switching reforming (GSR)*

The integration and techno-economic analysis of GSR with a gas-fired combined cycle power plant and CO<sub>2</sub> capture, a process designated as GSR-CC (gas switching reforming-combined cycle), was presented by Nazir, Cloete [15]. The GSR-CC process provides an opportunity for a flexible output, electricity or pure H<sub>2</sub>. The net electrical efficiency of the GSR-CC process presented by Nazir, Cloete [15] lies between 45-47.5%, which is competitive to that of other combined cycle power cycles with CO<sub>2</sub> capture, using steam-methane reforming at 43.6% [16], auto-thermal reforming at 46.9% [17] and chemical looping reforming between 42 -46% [18, 19]. The CO<sub>2</sub> avoidance in the GSR-CC is more than 95%, and is higher than any of the aforementioned methods.

Anyhow, there is still scope to optimize the GSR-CC process and improve its net electrical efficiency. The current paper evaluates different process integration options to reduce the efficiency penalty and simplify the process layout to make it more suitable for flexible operation. This paper addresses the gap in available literature on optimization of the GSR-CC process in terms of efficiency, and the proposed process can be a benchmark for other pre-combustion process concepts, particularly in the context of flexible operation for balancing wind and solar power. The remaining part of the paper contains the description of the improved process, methodology used for analysis and the results followed by conclusions.

## 2 Process improvement of GSR-CC

In this paper, seven different process cases and the respective net electrical efficiencies are presented and compared. The process cases cover the reference case natural gas combined cycle (NGCC) plant, the base case GSR-CC process, two cases using an improved gas turbine configuration and three cases for different heat integration options for the improved process. A brief description of the process cases is presented below.

### 2.1 Reference case

The reference case NGCC plant design is similar to the one specified in EBTF [20]. The NGCC comprises of two gas turbines (GT) and two heat recovery steam generators (HRSG) connected to a single steam turbine (ST) system. The ST system is a three-pressure level with one high pressure (HP) turbine, one medium pressure (MP) turbine and a two-flow low pressure (LP) turbine. The MP steam is reheated before being expanded in the MP turbine. The HRSG has a series of LP, MP and HP economizers, boilers and superheaters. The steam levels for LP/MP/HP steam are 3.4/33/166 bar at the inlet of the respective turbines. The GT system chosen is the GE 9371FB model since it is robust to fuel composition changes [15, 18, 20, 21].

### 2.2 Base case GSR-CC

The base GSR-CC process is similar to the one studied and presented in Nazir, Cloete [15], without the water-gas shift (WGS) step. The schematic of the GSR process is shown in Figure 1 and GSR-CC process is shown in Figure 2. Compressed air at 18 bar oxidizes the oxygen carrier (NiO on alumina support) resulting in a N<sub>2</sub>-rich stream during the oxidation step of the GSR. 12% of the air entering the GT is bled at compressor discharge of the GT, which is mixed with the compressed air from a separate air compressor. The oxygen carrier is reduced with the compressed off gas from PSA during the reduction step of the GSR and is then used as a catalyst for steam-methane reforming during the reforming step of the GSR. The steam used in reforming is superheated steam at 18 bar and 283 °C, which is taken from the MP steam turbine.

Syngas produced during the GSR reforming step is cooled and sent to PSA to separate out a 99.99% pure H<sub>2</sub> stream. The H<sub>2</sub> fuel is pre-heated and combusted for power generation in a combined cycle power plant. The reduction of the oxygen carrier with the PSA off-gas in the GSR produces a stream that contains only CO<sub>2</sub> and H<sub>2</sub>O, from which the H<sub>2</sub>O is condensed and the CO<sub>2</sub> stream is compressed and made ready for transport and storage. The CO<sub>2</sub> stream compression chain is similar to the one presented in EBTF [20]. The N<sub>2</sub>-rich stream from the oxidation step of the GSR is expanded in a turbine and cooled. A fraction of the N<sub>2</sub>-rich stream equal to the amount of the air bled from the GT is compressed and used as a diluent in the H<sub>2</sub> fuel combustion. Saturated HP steam is produced and sent to the HRSG while recovering heat from the cooling of syngas, CO<sub>2</sub> stream, N<sub>2</sub>-rich stream and inter-stage cooling of compressed N<sub>2</sub>-rich stream. Saturated LP steam is produced and sent to the HRSG while recovering heat from the N<sub>2</sub>-rich stream cooling at lower temperatures.



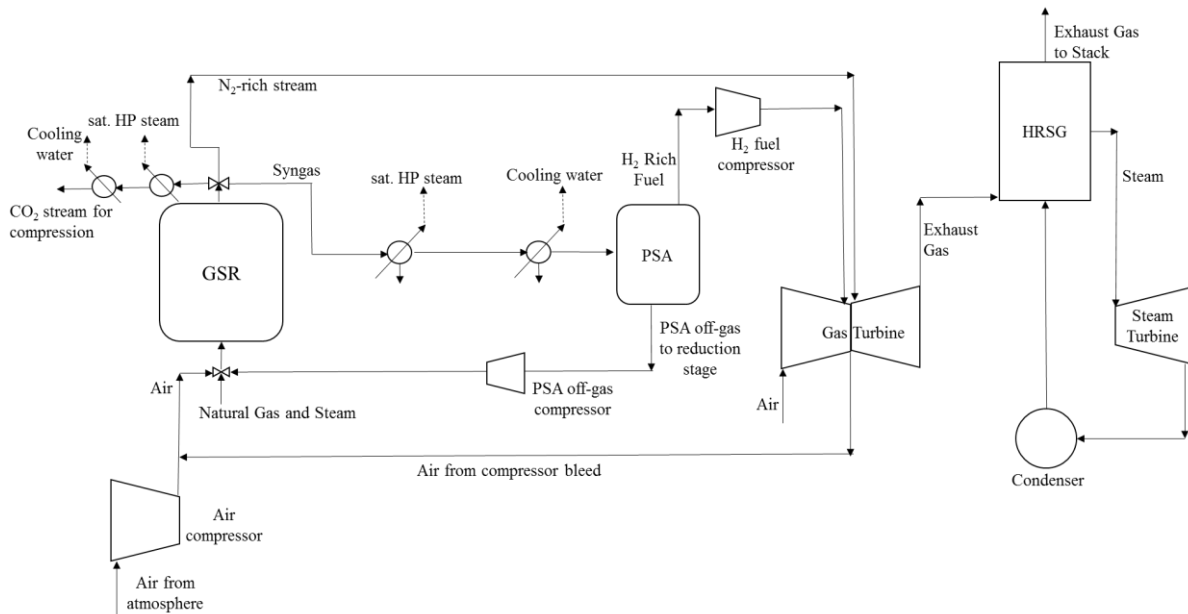


Figure 3: Schematic of improved GSR-CC process configuration

A conceptual illustration of the proposed LPM combustion chamber is shown in Figure 4. The LPM air/fuel mixture is fed to the combustion chamber and is brought into contact with the hot  $N_2$ -rich stream ( $\sim 1000^\circ C$ ) in the ignition zone where the high temperature of this stream ignites the air/fuel mixture. Secondary air is injected at the walls of the chamber to avoid excessive wall temperatures. The availability of the hot  $N_2$ -rich stream as ignition mechanism can allow the combustion chamber to be designed for flow velocities safely above the flame speed even at part-load operation without the risk of blowing out the flame under full load operation.

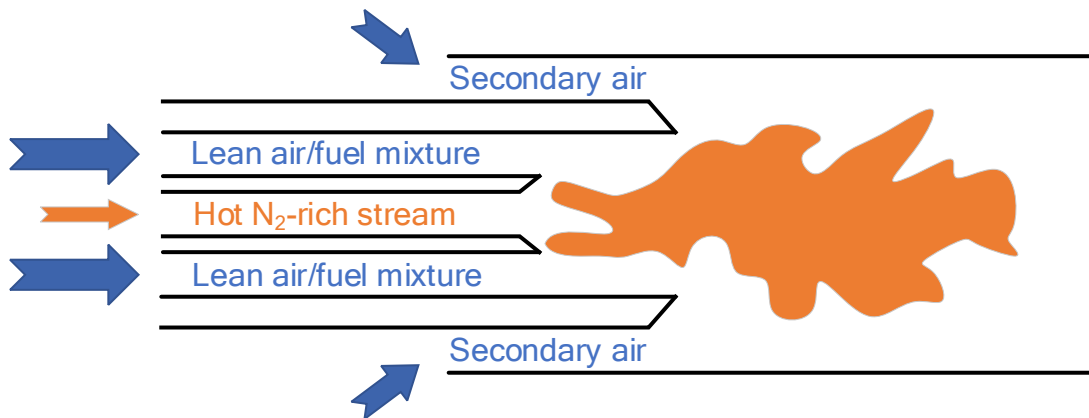


Figure 4: Conceptual illustration of the proposed LPM combustion chamber for fuel combustion with low  $NO_x$  formation.

In addition to the main benefit of allowing for high turbine inlet temperatures without high  $NO_x$  emissions, this LPM combustion chamber does not require high-pressure fuel injection. Hence, while the ratio of fuel pressure and compressor discharge in the GT is 1.65 in the base case, the fuel pressure is assumed to be equal to the combustor pressure in the improved GSR-CC case. Hence, the compression work in the  $H_2$  fuel compressor is less. This configuration also allows the total  $N_2$ -rich stream to flow from the GSR directly to the combustion chamber, therefore eliminating the steps of expansion, cooling and compression of  $N_2$ -rich stream as in the base case.



HRSG. The syngas is cooled down to a temperature of 65 °C with cooling water before being sent to the PSA to separate H<sub>2</sub>.

The off-gas from the PSA is compressed and pre-heated to 1000 °C in heat exchanger Hex 3 using the heat from the CO<sub>2</sub> stream from the GSR reduction step. The CO<sub>2</sub> stream is further cooled in heat exchanger Hex 5 to produce saturated HP steam, which is sent to the HRSG. The H<sub>2</sub>O in the CO<sub>2</sub> stream is condensed and the CO<sub>2</sub> stream is compressed to 110 bar to be ready for transport and storage. The air needed in the oxidation step of the GSR significantly reduces because of heat integration and hence there is no need for a separate air compressor.

Cases 4 and 5 aim to decouple the GSR process from the HRSG for improved operating flexibility. This presents the challenge of producing the steam required by the GSR process from the lower-grade heat remaining in the CO<sub>2</sub> and syngas streams after pre-heating the inlet gases to high temperatures in Hex 1 and Hex 3. This challenge is overcome by designing Hex 5 as a two-phase flow heat exchanger, where NG mixed with liquid water at 18.4 bar (considering 0.4 bar pressure drop in the heat exchanger) is heated with the CO<sub>2</sub> stream coming out of Hex 3. Feeding liquid water with natural gas allows water evaporation at lower temperatures because the presence of a dry gas reduces the steam partial pressure in the resulting gas mixture. As illustrated later in the results and discussion section, such a heat exchanger can generate most of the required steam by efficiently utilizing almost all of the condensation enthalpy in the steam in the CO<sub>2</sub> stream. The remaining steam required by the GSR process is raised in Hex 4.

In case 5, the process configuration is similar to case 4 except that heat exchanger Hex 2 produces steam for reforming at 18 bar, and heat exchanger Hex 4 is a two-phase flow heat exchanger where compressed H<sub>2</sub> stream is mixed with liquid water and is heated by the syngas coming from heat exchanger Hex 2. The presence of steam with the pre-heated H<sub>2</sub> will slightly reduce the air compression work requirement and further reduce NO<sub>x</sub> formation in the turbine.

Case 5 is designed for maximum flexibility to alternate (or blend) between H<sub>2</sub> and power production modes. In H<sub>2</sub> production mode, Hex 4 will simply use cooling water to cool the syngas stream to the PSA unit, while the pure H<sub>2</sub> is kept at a low temperature for subsequent compression. Hex 4 will only operate to pre-heat hydrogen and generate some additional steam during power production mode, using low-grade heat that is wasted when the plant is operating in H<sub>2</sub> production mode. Under part-load operation, the plant has the flexibility to only heat up the part of the produced H<sub>2</sub> required in the gas turbine in Hex 4, while the remainder is sent to the H<sub>2</sub> compressors.

The methodology used for process analysis is described in the next section.

### **3 Methodology and Assumptions**

The transient behavior of the GSR reactor is simulated using a 0D model developed using Matlab R2018a, which solves the mole and energy balances of the reactor. The primary assumptions of the model are that the reactor behavior can be approximated as that of a continuous stirred tank reactor (CSTR) and that thermal and chemical equilibrium is reached within the reactor. These are reasonable assumptions considering the excellent mixing provided

by fluidized bed reactors and the large dimensions of the industrial-scale devices considered here. Specifically, the CSTR assumption is supported by earlier work where reactor simulations with a CSTR model [24] gave similar results to simulations using a detailed computational fluid dynamics model [25]. The thermal and chemical equilibrium assumption is supported by experimental studies showing that equilibrium conversion can be achieved even in a lab-scale GSR reactor [26] with much smaller gas residence time than the industrial reactors considered in this study. The balance equations that are solved, as well as the chemical reactions considered, are identical to that of a previous study [12] and are therefore not repeated here.

Due to the recycling of the PSA off-gas to the GSR reactor, the coupling between the reactor and plant simulations is done manually using the following procedure: The inlet stream temperatures are provided by the plant scale model, as well as the composition and flow rate of the inlet stream to the reforming stage. An estimate is used for the conditions of the PSA off-gas fed to the reduction stage. The reactor simulations are then performed by automatically controlling the air flow rate to the oxidation stage to maintain a maximum temperature of 1100 °C in the cycle. The required air flow rate, as well as the composition, flow rate and temperature of the syngas produced in the reforming stage is then provided to the plant scale model. The plant scale simulation is repeated to update the flow rate and composition of the PSA off-gas delivered to the reactor during the reduction stage. Another iteration of the reactor simulation is then performed to obtain the conditions of all the reactor outlet streams for use in the plant scale model.

Aspen Hysys V8.6 [27] and Thermoflex component of the Thermoflow Suite V26 [28] were used to model the process. The N<sub>2</sub>-rich stream treatment, syngas treatment and cooling, PSA off-gas compression and cooling, CO<sub>2</sub> stream cooling and compression were modeled in Aspen Hysys V8.6. Peng-Robinson model was used to estimate the thermodynamic properties [15, 29]. The H<sub>2</sub> stream compression and the power plant were modeled in Thermoflex. The PSA was modeled as a 'black box' assuming 86% recovery of H<sub>2</sub> with 99.99% purity [30, 31].

The reference case NGCC plant is modeled very similar to the methodology mentioned in the EBTF [20] for a NGCC plant without CO<sub>2</sub> capture. The NG is assumed to be 100% CH<sub>4</sub> for the analysis in this paper. The net electrical efficiency of such a NGCC plant is 58.3% on lower heating value (LHV) basis. The base case GSR-CC plant is modeled similar to the process configuration presented in Nazir, Cloete [15] for the GSR-CC without WGS. The design pressure in the GSR is maintained 18 bar in all the cases since this pressure was found to be an optimum fit when pressurized fluidized bed reformers are integrated for power generation purposes [19]. In the base case GSR-CC presented in this paper, the heat of condensation of steam in the syngas and the CO<sub>2</sub> stream is discarded in the cooling water. The pressure drop in the heat exchangers are assumed 0.4 bar for liquid stream and 2% for a gaseous stream. In the WGS, 3% pressure drop is assumed. The H<sub>2</sub> stream from the PSA comes out at a 0.2 bar lower pressure than the PSA-inlet stream and has a flow of 46.35 TPH in all the cases. Additional NG is added to the PSA off-gas if the oxygen carrier is not reduced completely by the PSA off-gas in the reduction step of the GSR. The polytropic efficiency of the N<sub>2</sub> stream turbine is assumed 83%, to maintain consistency with the performance of the turbine in the GE 9371FB system.

In case 1 and 2, the S/C ratio in the reforming step of the GSR is 1.6, whereas it is 2 in the case 3, 4 and 5. In case 1-5, the GT system is a generic model and not the standard commercial GE 9371FB GT as considered in the reference case and the base case GSR-CC. The performance

of the GT system components in cases 1-5 is consistent with the performance of the GE 9371FB model, i.e. by assuming the polytropic efficiency of the compressor and turbine as 90% and 83% respectively. In case 1, the flowrate of air in the GSR and the GT system is similar to the base case GSR-CC, while the air flowrate to the GT is tailored to maintain a TIT close to 1433 °C in the remaining cases. In the base case, case 1, case 2 and case 3, the saturated HP and LP steam produced during heat recovery is at 174.4 and 3.8 bar respectively (similar to the pressure at the respective boiler outlet in the HRSG), which is then mixed with the saturated steam from the HP and LP boiler in the HRSG system, before being superheated and sent to the ST.

In case 4 and 5, the steam for reforming is produced by recovering heat from the syngas and the CO<sub>2</sub> stream. In case 4, nearly 99 TPH saturated steam at 18 bar for reforming is prepared in Hex 4 (Figure 5). In case 5, nearly 99 TPH saturated steam at 18 bar for reforming is prepared in Hex 2 (Figure 5). In case 5, the remaining heat in the syngas coming out from Hex 2 is recovered in a two-phase flow heat exchanger where a mixture of H<sub>2</sub> stream and water is heated to vaporize the water. The amount of water vaporized is 1.94 TPH for every 1 TPH H<sub>2</sub> stream flowrate. The resulting temperature of the H<sub>2</sub> stream and steam mixture is 260 °C.

The net electrical efficiency ( $\eta$ ) and the CO<sub>2</sub> avoidance are estimated for the cases defined and are calculated using in Eq. 1 and Eq. 2

$$\begin{aligned} & \text{Net Electrical Efficiency } (\eta) \\ & = \frac{100 \times \text{Net electricity produced in GSR-CC process}}{\text{LHV of NG input to the process}} \end{aligned} \quad \text{Eq. 1}$$

$$\begin{aligned} & \text{CO}_2 \text{ Avoidance } (\%) \\ & = \frac{100 \times (\text{CO}_2 \text{ emitted in NGCC} - \text{CO}_2 \text{ emitted in GSR-CC})}{\text{CO}_2 \text{ emitted in NGCC}} \end{aligned} \quad \text{Eq. 2}$$

## 4 Results and Discussion

The syngas composition for the cases is shown in Table 1. The main operating conditions in the GSR unit for the different cases are shown in Table 2. Table 3 shows the main results for the process improvement and heat integration in GSR-CC and compares them to the results for the base case GSR-CC and the reference case NGCC power plant. In Table 3, the power consumed or produced in any component is represented as a percentage of the NG fuel input (LHV) to the process. A negative sign signifies that power is consumed by the component.

The temperatures during the oxidation, reduction and reforming steps of the GSR are higher in the cases of heat integration. This is because the heat recovered from the syngas and CO<sub>2</sub> stream from the GSR is recirculated back to the GSR through pre-heating of inlet streams during the reduction and reforming steps. As seen in Figure 6, the higher inlet temperatures lead to a smaller drop in the reactor temperature during the reduction (0-300s) and reforming (300-900s)

stages compared to the cases without heat integration. This, in turn, results in higher average temperatures during each of the stages, considering that the maximum temperature in the cycle is always fixed to 1100 °C.

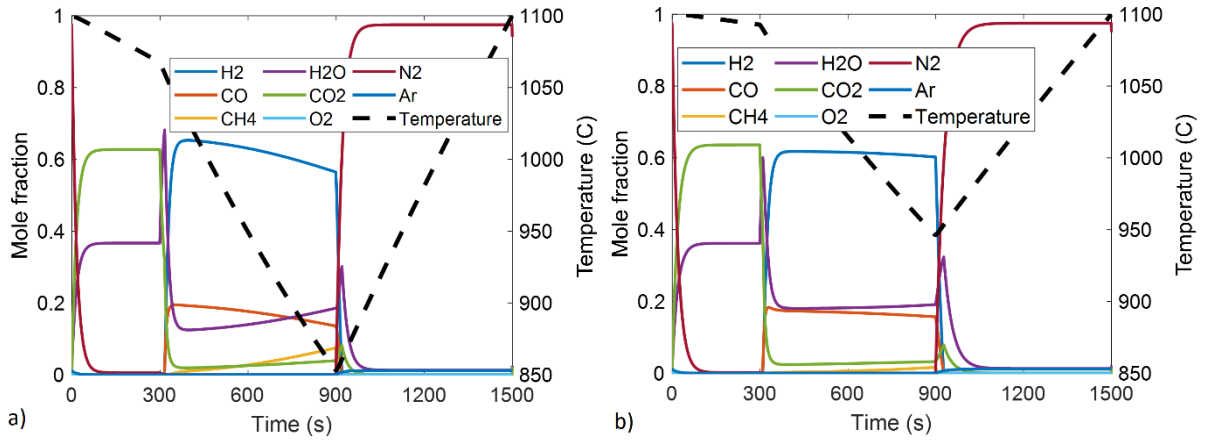


Figure 6: The composition and temperature at the reactor outlet during a cycle for a) the cases with improved GSR-CC and without heat integration and b) the cases with improved GSR-CC and heat integration.

The GSR concept combusts PSA off-gas to drive the endothermic reforming reactions and to heat up the incoming gases. When the inlet streams to the reduction and reforming stages are pre-heated, less PSA off-gas is required to raise the temperature of these inlet streams to the reactor temperature. In Table 2, the lower amount of fuel combustion required is best observed through the large reduction in the required air flowrate to the oxidation step when heat integration is included (cases 3, 4 and 5). This lower flowrate of air over the fixed stage time is the reason for the lower degree of oxygen carrier utilization reported for the heat integration cases in Table 2. The heat integration results in lesser specific NG consumption to produce the fixed flowrate of H<sub>2</sub> fuel, as observed in cases 3, 4 and 5.

Table 1: Syngas composition in different cases

Cases / Component	Base case, case 1 and case 2	Case 3, case 4 and case 5
H <sub>2</sub> O	0.15	0.20
CO <sub>2</sub>	0.04	0.03
CH <sub>4</sub>	0.02	0.01
CO	0.17	0.17
H <sub>2</sub>	0.62	0.59

Table 2: Design conditions in the GSR for different cases

Cases	Units	Base case, case 1 and case 2	Case 3, case 4 and case 5
Oxidation step			
Oxygen carrier utilization	%	33	20
Outlet Temperature	°C	980	1027
Air flowrate	TPH	1166	693
N <sub>2</sub> -rich stream flowrate	TPH	900	530
Reduction Step			
Outlet temperature	°C	1082	1096
PSA off-gas flowrate	TPH	317	320
PSA off-gas temperature at inlet of GSR	°C	409	1000
Reforming Step			
Steam/Carbon		1.6	2
NG Flowrate	TPH	159	133
Outlet Temperature	°C	949	1018
H <sub>2</sub> O/CO in syngas	mol/mol	0.88	1.2
NG and H <sub>2</sub> O temperature at inlet of GSR	°C	183	890

Process configuration improvement and heat integration in the GSR-CC plant has a significant effect on the net electrical efficiency. As shown in Table 3, the net electrical efficiency of the base case GSR-CC process is 45.8%, which is ~12.5%-points less than the reference NGCC plant. The main efficiency penalty comes in gas turbine. Compared to the gas turbine output of 37.7% LHV fuel input in the reference NGCC plant, the net generation from the gas turbines and compressors (including N<sub>2</sub>-rich stream expansion and compression) in the base case is only 27.1% LHV fuel input. This large drop in gas turbine output is partially offset by a small increase in the steam turbine output since additional steam is produced in heat recovery from the syngas, N<sub>2</sub>-rich stream and CO<sub>2</sub> stream from the GSR unit. It is therefore clear that the base case puts less energy through the topping cycle and more through the bottoming cycle, leading to a large efficiency penalty relative to the reference case. Other significant penalties come from the H<sub>2</sub> compressor to inject fuel into the gas turbine, the PSA off-gas compressors required because of the pressure swing H<sub>2</sub> separation process, and the unavoidable CO<sub>2</sub> compression required by CCS plants.

In case 1, the net electrical efficiency of the GSR-CC process is 1.6 %-points more than the base case. Significant improvement is seen in the power produced by the gas turbine system in case 1 since all the N<sub>2</sub>-rich stream is recirculated back into the GT at a higher temperature. Hence, the N<sub>2</sub>-rich stream is directly expanded in the GT and not in a separate N<sub>2</sub>-rich stream turbine as in the base case. The net power generation from the gas turbine and additional air compressor in this case is 27.7% of LHV fuel input, which is 0.6 %-points higher than the base case. In addition, the efficiency penalty due to the H<sub>2</sub> fuel compression is now almost zero because the ratio of fuel pressure to the compressor discharge pressure in the GT (combustor inlet pressure) is assumed to be 1 due to pre-mixing of fuel and air. The auxiliary power consumption reduces in case 1 with respect to the base case, since the process steps to treat N<sub>2</sub>-rich stream is not present in case 1. Since more N<sub>2</sub> is now fed to the gas turbine and the air flowrate is kept constant, the TIT in the case 1 reduces to 1347 °C relative to 1433 °C in the base case.

In case 2, the net electrical efficiency of the process improves by 1.1 %-points when compared to the case 1, by increasing the TIT close to 1433 °C as implemented in base case. The TIT is increased by increasing the air bled from the compressor discharge of the GT from 12% to 22.5%. This reduces the amount of power produced from the GT since the mass flow rate through the GT has reduced when compared to case 1. However, increasing the air bled from the GT system reduces the amount of additional air compression before the oxidation step of the GSR, resulting in a net generation from the turbine and air compressor of 28.1 % of LHV fuel input, which is 0.4 %-points more than case 1. A larger power production increase of 0.7 %-points is observed for the steam turbine due to the higher turbine outlet temperature. The remaining efficiency penalties remain the same.

Table 3: Main results for improvement of GSR-CC process

Cases	Units	Ref. case (NGCC without capture)	Base case GSR -CC	GSR-CC with improved GT configuration		GSR-CC with heat integration		
				1	2	3	4	5
Gas Turbine	% - LHV	37.7	27.3	31.0	28.8	33.9	34.0	34.6
Steam Turbine	% - LHV	21.9	23.8	24.0	24.7	20.8	21.2	21.1
N <sub>2</sub> -rich Stream Turbine	% - LHV	-	7.4	-	-	-	-	-
Diluent N <sub>2</sub> Stream Compressor	% - LHV	-	- 4.3	-	-	-	-	-
H <sub>2</sub> fuel Compressor	% - LHV	-	- 0.7	- 0.1	- 0.1	- 0.3	- 0.3	- 0.3
Air Compressor	% - LHV	-	- 3.3	- 3.3	- 0.7	-	-	-
PSA off-gas compressor	% - LHV	-	- 2.2	- 2.2	- 2.2	- 2.3	- 2.3	- 2.3
CO <sub>2</sub> Compressors and Pump	% - LHV	-	- 1.0	- 1.0	- 1.0	- 1.0	- 1.0	- 1.0
Auxiliaries	% - LHV	- 1.3	- 1.2	- 1.0	- 1.0	- 1.0	- 1.0	- 1.0
Net LHV Input to process	MW	1513	2215	2215	2215	1851	1847	1851
Net Electrical Efficiency	% - LHV	58.3	45.8	47.4	48.5	50.1	50.6	51.1
CO <sub>2</sub> Avoidance	%	-	96.4	96.4	96.9	98.1	98.1	98.1
CO <sub>2</sub> Capture	%	-	97.5	97.5	97.9	98.7	98.7	98.7

In case 3, the heat integration of the process streams to pre-heat the inlet streams to reduction and reforming steps increases the net electrical efficiency by 1.6 %-points with respect to case 2. The significant difference in efficiency comes mainly from the large increase in power produced in the GT. Instead of recovering heat in the syngas and CO<sub>2</sub> stream to produce steam that is sent to HRSG, the reduction and reforming step inlets are pre-heated alongside pre-heating the H<sub>2</sub> fuel going to the GT system. This allows for a higher fraction of energy

throughput in the GT. Air needed in the oxidation step of the GSR is nearly 60% of what is required in the base case, case 1 and case 2. Hence, 15% of the air bled from the compressor discharge in the GT system is enough for the oxidation step and an additional air compressor is not required. Due to these factors, the GT power output at 33.9% of LHV fuel input is fully 5.8 %-points more than case 2. However, since less steam is now produced from the GSR outlet streams and sent to the HRSG, the power produced from the ST is 3.9 %-points lower when compared to case 2. The H<sub>2</sub> compressor consumption also increased due to a reduction in H<sub>2</sub> pressure from the PSA. An additional WGS step and increased number of heat exchangers in case 3 when compared to case 2 resulted in larger pressure losses in the syngas stream entering the PSA unit.

Case 4 experiences a net electrical efficiency increase by 0.5%-points with respect to case 3. Here, the steam for reforming is produced by recovering heat from the syngas and CO<sub>2</sub> streams. Hence, the steam for reforming need not be extracted from the MP steam turbine and the power produced from the ST is 0.4 %-points higher in case 4 when compared to case 3. It is noteworthy that the plant efficiency can be improved while eliminating the coupling between the GSR system and the HRSG to improve operating flexibility of the plant.

In case 5, the net electrical efficiency of the GSR-CC process is 0.5%-points more than in case 4 and 5.3%-points more than the base case. In case 5, the heat from the syngas is completely recovered by heating up a mixture of H<sub>2</sub> fuel and water, by vaporizing the water. The mixture of H<sub>2</sub> fuel and steam is then sent to the GT system requiring a smaller amount of air compression work. Therefore, the power output from the GT in case 5 is 0.6 %-points higher than in case 4.

Cases 4 and 5 are dependent on two-phase flow heat exchangers where liquid water is mixed with a gas at the cold side inlet. Given that the liquid volume fraction will only be in the order of 1%, this water could be injected into the cold stream via an atomizer upstream of the heat exchanger so that the resulting fine mist of liquid droplets will be evenly distributed at the inlet of the heat exchanger. The temperature profiles in these heat exchangers were simulated using a simplified 1D heat transfer model in ANSYS FLUENT v16.2.

As shown in Figure 7a, the heat exchanger cooling the CO<sub>2</sub>-rich stream (Hex 5 in Figure 5) could exploit essentially all the steam condensation enthalpy in the CO<sub>2</sub>-rich stream to raise steam for the reforming (the hot stream is cooled to room temperature). The point where steam condensation starts is clearly visible after about 50% of the heat is transferred. Even though the temperature difference between the hot and cold streams is relatively small after this point, the heat transfer coefficient will be high because phase change is happening in both streams, thereby limiting the required heat exchange surface area.

Figure 7b shows that not all the steam condensation enthalpy could be recovered from the syngas stream via Hex 4 in Figure 5 (the hot stream could only be cooled to 85 °C). Still, 72% of the steam condensation enthalpy in this stream could be recovered to raise steam to be fed with the H<sub>2</sub> to the combustion chamber, creating an efficiency gain of 0.5 %-points as outlined above.

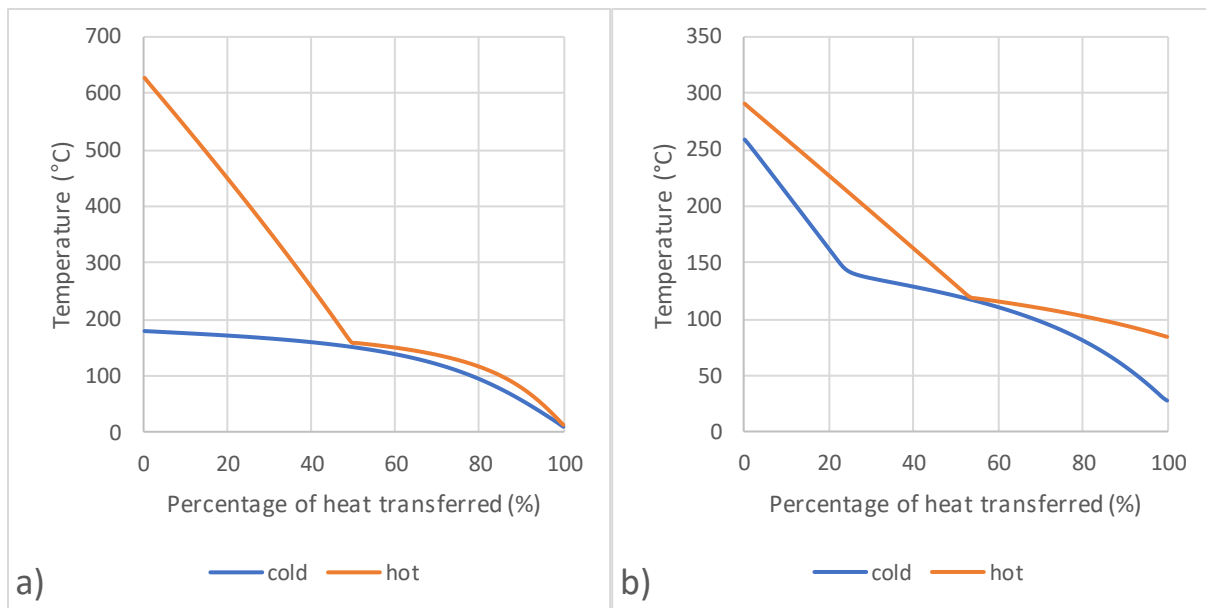


Figure 7: Temperature profiles in the two-phase flow heat exchangers: a) heat transfer from the CO<sub>2</sub>-rich stream to the reforming inlet stream and b) heat transfer from the syngas stream to the hydrogen stream.

Case 5 shows an efficiency penalty of only 7.2 %-point when compared to reference NGCC plant with more than 95% CO<sub>2</sub> avoided. This outperforms post-combustion CO<sub>2</sub> capture systems with 7.6-8.4 %-point energy penalty and 88% CO<sub>2</sub> avoidance [32, 33].

Almost the entirety of the GSR-CC energy penalty is related to the conversion of NG to H<sub>2</sub>, particularly the need to raise steam for the NG reforming reaction. Since the produced H<sub>2</sub> is combusted in a combined cycle, the condensation enthalpy of the resulting steam cannot be recovered, implying that all energy used to raise steam for reforming is lost for the purpose of producing useful work. In case 5, 298 TPH of steam needs to be raised, requiring 187 MW of heat – about 10% of LHV fuel input. If the power cycle efficiency is assumed to be 58%, this translates to a 5.8 %-points loss in net electric efficiency. Other losses include 1 %-point from CO<sub>2</sub> compression and 2.3 %-points from the PSA off-gas compressor, although the electrical energy input to the latter is directly integrated into the process by heating the PSA off-gas stream, meaning that the actual energy penalty is also around 1 %-point. On the positive side, the latent heat recovery from 85 TPH of steam in the CO<sub>2</sub> stream and 65 TPH of steam in the syngas stream via the two-phase flow heat exchangers improves the overall electrical efficiency.

Given that the primary added value of the GSR-CC process is in the conversion of NG to H<sub>2</sub> with integrated CO<sub>2</sub> capture and not in the conversion of the resulting H<sub>2</sub> to electricity, the flexibility of the process to produce either product is very important. As a power plant, it would be more efficient to use gas switching combustion (GSC) [24] to convert NG to high grade heat for power production with integrated CO<sub>2</sub> capture without any of the losses related to H<sub>2</sub> production. However, GSC also faces efficiency challenges from the maximum temperature limitation of the reactors and downstream valves, and will require additional fuel combustion after the reactors to reach the operating temperatures achievable by modern gas turbines.

Despite the efficiency penalty of H<sub>2</sub> production, the ability of GSR-CC to produce clean H<sub>2</sub> continuously and only convert this H<sub>2</sub> to electricity during times when the electricity price becomes high enough promises to be a major benefit in a future energy system with high shares

of variable wind and solar power. Future work will therefore investigate the part-load and H<sub>2</sub>-only operating modes of the GSR-CC plant.

In practice, the power cycle in the GSR-CC plant will operate flexibly in response to wholesale electricity price signals just like NGCC plants operate today. The primary difference is that the H<sub>2</sub>-production train will keep on producing H<sub>2</sub> for export during times when the power cycle is shut down because wholesale electricity prices are too low for profitable operation.

It should be mentioned that such a flexible GSR-CC plant will require stronger demand for H<sub>2</sub> than is the case today to facilitate large-scale H<sub>2</sub> exports during times of low electricity prices. The cheap electricity available at this time will be used to economically compress H<sub>2</sub> to high pressures to facilitate more efficient distribution and storage of the produced clean energy carrier for use in transportation or industrial applications.

Another possibility is to store the H<sub>2</sub> produced during periods of low electricity prices on site for combustion in the power cycle during times of high electricity prices. In this case, the H<sub>2</sub>-production train (GSR, WGS, PSA and CO<sub>2</sub> compression) can be sized for the expected average plant load, whereas the power cycle is sized for maximum load. H<sub>2</sub> storage tends to be relatively expensive, so this option may require the plant to be situated at a suitable underground formation that facilitates low-cost H<sub>2</sub> storage [34]. Future economic assessments will better quantify the trade-offs involved in this configuration.

## 5 Conclusions

This paper focused on the improvements in the GSR-CC process [15], which comprises of a novel gas switching reforming (GSR) process for hydrogen production with integrated CO<sub>2</sub> capture linked to a combined cycle to generate electricity from the produced H<sub>2</sub>. It was concluded from the previous works in the field of chemical looping and gas switching concepts that the fuel cost contributes most to the cost of electricity. The fuel cost (NG cost) accounts for 40% increase in the levelised cost of electricity (with respect to reference NGCC plant), whereas 35% increase comes from additional equipment for pre-combustion capture and 25% increase comes from the larger equipment costs due to efficiency penalty in the GSR-CC [15, 18]. A similar trend is noticed in chemical looping reforming based combined cycle [12, 18]. The energy penalty is therefore responsible for as much as two thirds of the increase in levelised cost of electricity in these pre-combustion power plants (increased fuel consumption and larger equipment sizes required). Hence, process efficiency was increased via process configurations with an improved lean pre-mixed combustion turbine and a smaller number of unit operations as well as improved heat integration between the inlet and outlet streams of the GSR process. The improved GSR-CC process configuration also has a smaller number of unit operations, thereby restricting the increase in the capital requirement for pre-combustion capture.

Two cases for improved process configuration and three cases for heat integration were presented. The cases with the improved gas turbine configuration allowed for the direct injection of the hot N<sub>2</sub>-rich stream from the GSR oxidation stage into the combustion chamber, where it can aid in controlling the lean pre-mixed combustion. Heat integration in the GSR

process allowed more of the incoming fuel to be converted to H<sub>2</sub> instead of simply heating up the inlet streams to the reactor temperature.

The net electrical efficiency of the GSR-CC process was improved from 45.8% in the base case to 51.1% in the optimal case. A gain of 2.7%-points in the net electrical efficiency of the GSR-CC is obtained from changes in gas turbine configuration whereas an additional 2.6%-point gain comes from improved heat integration. The improved GSR-CC process has an efficiency penalty of 7.2 %-points and CO<sub>2</sub> avoidance of more than 95% with respect to the reference case NGCC plant without CO<sub>2</sub> capture. It outperforms NGCC plants with amine based post-combustion capture both in terms of efficiency and CO<sub>2</sub> avoidance [33]. The other advantage of the GSR-CC plant is that the output is flexible in terms of pure H<sub>2</sub> or electricity. The optimal plant configuration was designed to maximize this flexibility, which will be valuable in a future scenario with high market shares of variable wind and solar power.

## Acknowledgements

The current work is part of “GaSTech” project under the Horizon 2020 programme, ACT Grant Agreement No 691712. The authors appreciate the funding authorities, Research Council of Norway and the European Commission. The authors also appreciate the project partners in GaSTech.

## References

1. IEA, *Key World Energy Statistics 2017*. 2017.
2. ETP, *Energy Technology Perspectives*. 2017, International Energy Agency.
3. WEO, *World Energy Outlook 2016*. 2016, International Energy Agency.
4. ClimateFocus, *The Paris Agreement: Summary*. 2015. p. 1-6.
5. Boot-Handford, M.E., et al., *Carbon capture and storage update*. Energy and Environmental Science, 2014. **7**(1): p. 130-189.
6. Kenarsari, S.D., et al., *Review of recent advances in carbon dioxide separation and capture*. RSC Advances, 2013. **3**(45): p. 22739-22773.
7. GCCSI, *The Global Status of CCS: 2017*. 2017, Global CCS Institute.
8. Lyngfelt, A., B. Leckner, and T. Mattisson, *A fluidized-bed combustion process with inherent CO<sub>2</sub> separation; application of chemical-looping combustion*. Chemical Engineering Science, 2001. **56**(10): p. 3101-3113.
9. Ishida, M., D. Zheng, and T. Akehata, *Evaluation of a chemical-looping-combustion power-generation system by graphic exergy analysis*. Energy, 1987. **12**(2): p. 147-154.
10. Rydén, M., A. Lyngfelt, and T. Mattisson, *Synthesis gas generation by chemical-looping reforming in a continuously operating laboratory reactor*. Fuel, 2006. **85**(12-13): p. 1631-1641.
11. Adanez, J., et al., *Progress in chemical-looping combustion and reforming technologies*. Progress in Energy and Combustion Science, 2012. **38**(2): p. 215-282.
12. Nazir, S.M. and O. Bolland, *Techno-economic analysis of combined cycle power plants integrated with chemical looping reforming and CO<sub>2</sub> capture*, in *Department of Energy and Process Engineering*. 2018, Norwegian University of Science and Technology: Trondheim. p. 217.
13. Wassie, S.A., et al., *Hydrogen production with integrated CO<sub>2</sub> capture in a novel gas switching reforming reactor: Proof-of-concept*. International Journal of Hydrogen Energy, 2017. **42**(21): p. 14367-14379.

14. Zaabout, A., et al., *Experimental Demonstration of a Novel Gas Switching Combustion Reactor for Power Production with Integrated CO<sub>2</sub> Capture*. *Industrial & Engineering Chemistry Research*, 2013. **52**(39): p. 14241-14250.
15. Nazir, S.M., et al., *Techno-economic assessment of the novel gas switching reforming (GSR) concept for gas-fired power production with integrated CO<sub>2</sub> capture*. *International Journal of Hydrogen Energy*, 2018. **43**(18): p. 8754-8769.
16. Lozza, G. and P. Chiesa, *Natural Gas Decarbonization to Reduce CO<sub>2</sub> Emission From Combined Cycles—Part II: Steam-Methane Reforming*. *Journal of Engineering for Gas Turbines and Power*, 2000. **124**(1): p. 89-95.
17. Kvamsdal, H.M., K. Jordal, and O. Bolland, *A quantitative comparison of gas turbine cycles with CO<sub>2</sub> capture*. *Energy*, 2007. **32**(1): p. 10-24.
18. Nazir, S.M., et al., *Techno-economic assessment of chemical looping reforming of natural gas for hydrogen production and power generation with integrated CO<sub>2</sub> capture*. *International Journal of Greenhouse Gas Control*, 2018. **78**: p. 7-20.
19. Nazir, S., O. Bolland, and S. Amini, *Analysis of Combined Cycle Power Plants with Chemical Looping Reforming of Natural Gas and Pre-Combustion CO<sub>2</sub> Capture*. *Energies*, 2018. **11**(1): p. 147.
20. EBTF, *European best practice guidelines for assessment of CO<sub>2</sub> capture technologies. CESAR -project 7th FrameWork Programme. Collaborative Project— GA No. 213569*. 2011.
21. Nord, L.O., R. Anantharaman, and O. Bolland, *Design and off-design analyses of a pre-combustion CO<sub>2</sub> capture process in a natural gas combined cycle power plant*. *International Journal of Greenhouse Gas Control*, 2009. **3**(4): p. 385-392.
22. Chiesa, P., G. Lozza, and L. Mazzocchi, *Using Hydrogen as Gas Turbine Fuel*. *Journal of Engineering for Gas Turbines and Power*, 2005. **127**(1): p. 73-80.
23. Andersen, T., H. M. Kvamsdal, and O. Bolland, *Gas Turbine Combined Cycle With CO<sub>2</sub> - Capture Using Auto-Thermal Reforming of Natural Gas*. 2000.
24. Cloete, S., et al., *Integration of a Gas Switching Combustion (GSC) system in integrated gasification combined cycles*. *International Journal of Greenhouse Gas Control*, 2015. **42**: p. 340-356.
25. Cloete, S., et al., *Optimization of a Gas Switching Combustion process through advanced heat management strategies*. *Applied Energy*, 2017. **185**: p. 1459-1470.
26. Wassie, S.A., et al., *Hydrogen production with integrated CO<sub>2</sub> capture in a membrane assisted gas switching reforming reactor: Proof-of-Concept*. *International Journal of Hydrogen Energy*, 2018. **43**(12): p. 6177-6190.
27. AspenHYSYS, *Aspen HYSYS V8.6 User Guide*. 2017, Aspen Technology Inc., Bedford, Massachusetts, USA.
28. Thermoflow, *Thermoflow Suite V26 User Guide*. 2017, Thermoflow Inc., Southborough, MA, USA.
29. Nazir, S.M., O. Bolland, and S. Amini, *Full Plant Scale Analysis of Natural Gas Fired Power Plants with Pre-Combustion CO<sub>2</sub> Capture and Chemical Looping Reforming (CLR)*. *Energy Procedia*, 2017. **114**: p. 2146-2155.
30. Riboldi, L. and O. Bolland, *Overview on Pressure Swing Adsorption (PSA) as CO<sub>2</sub> Capture Technology: State-of-the-Art, Limits and Potentials*. *Energy Procedia*, 2017. **114**(Supplement C): p. 2390-2400.
31. Sircar, S. and T.C. Golden, *Purification of Hydrogen by Pressure Swing Adsorption*. *Separation Science and Technology*, 2000. **35**(5): p. 667-687.
32. Diego, M.E., J.-M. Bellas, and M. Pourkashanian, *Techno-economic analysis of a hybrid CO<sub>2</sub> capture system for natural gas combined cycles with selective exhaust gas recirculation*. *Applied Energy*, 2018. **215**: p. 778-791.
33. Sanchez Fernandez, E., et al., *Thermodynamic assessment of amine based CO<sub>2</sub> capture technologies in power plants based on European Benchmarking Task Force methodology*. *Fuel*, 2014. **129**: p. 318-329.
34. Le Duigou, A., et al., *Relevance and costs of large scale underground hydrogen storage in France*. *International Journal of Hydrogen Energy*, 2017. **42**(36): p. 22987-23003.

35. Spallina, V., et al., *Techno-economic assessment of membrane assisted fluidized bed reactors for pure H<sub>2</sub> production with CO<sub>2</sub> capture*. *Energy Conversion and Management*, 2016. **120**: p. 257-273.